American Mineralogist, Volume 61, pages 732–750, 1976

Limits to the assemblage forsterite–anorthite as inferred from peridotite hornfelses, Icicle Creek, Washington

B. Ronald Frost

Department of Geological Sciences, University of Washington[1]
Seattle, Washington 98195.

Abstract

Hornblende–plagioclase peridotite has formed in aluminous reaction zones around mafic lenses in chromite-bearing forsterite–enstatite–tremolite metaperidotite close to the contact of a gabbroic phase of the Mount Stuart Batholith. Assemblages encountered in these aluminous rocks are consistent with a theoretically-derived topology for the reactions governing the occurrence of plagioclase in peridotite, which indicates that the low-temperature limit of plagioclase peridotite in the pure system is the reaction 5 anorthite + 8 forsterite + 2 H_2O = 2 tremolite + diopside + 5 spinel.

Associated pelitic hornfelses contain assemblages which indicate that the metamorphism occurred at pressures between 2 and 4 kilobars. The reaction chlorite = forsterite + enstatite + spinel + H_2O, which occurs in the metaperidotite near the contact with the batholith, establishes that the temperature at the time of metamorphism reached 715 ± 25°C. Only in a small pendant enclosed within the gabbro do mafic hornfelses contain the assemblage hornblende–clinopyroxene–orthopyroxene–plagioclase, indicative of transition to pyroxene–hornfels facies.

The reaction-zone rocks contain assemblages which are indicative of both sides of the reaction 2 forsterite + anorthite = enstatite + diopside + spinel, with the enstatite and diopside-bearing assemblages containing spinel richer in chromite than the forsterite + anorthite-bearing assemblages. Thermodynamic calculations using observed spinel compositions suggest pressures at least 2 kilobars below the pressure inferred from the pelitic assemblages. It is argued that the main cause for this discrepancy is error in the assumption of ideality in the spinel solid solution.

Hornblende in the hornblende–plagioclase peridotite is colorless and shows a systematic variation in alkali content and tetrahedral aluminum along a trend rich in the tschermakite endmember. By expressing this compositional change mathematically, diagrams are derived which show that for the hornblende compositions used, the low-pressure peridotites can be divided into three chlorite-free mineral facies. They are, in increasing grade, hornblende–spinel peridotite, hornblende–plagioclase peridotite, and finally plagioclase lherzolite.

Introduction

Models for the mineralogy of aluminous lherzolite, based upon experimental work (Kushiro and Yoder, 1966; Emslie, 1970; Green and Hibberson, 1970; and Herzberg, 1972) indicate a fairly wide stability field for plagioclase in peridotite at high temperatures and relatively low pressures (*cf.* O'Hara, 1967a). Although plagioclase + olivine is a common magmatic assemblage and plagioclase peridotite of clearly magmatic origin does occur (*cf.* Brown, 1956; Leake, 1964; Onuki, 1965; and Irvine and Smith, 1967), plagioclase peridotite from low-pressure regionally-metamorphic or contact-metamorphic environments has not been reported. Plagioclase and olivine-bearing assemblages have been described from basaltic rocks which have been subjected to metamorphism in pyroxene hornfels facies (Richey and Thomas, 1930; MacGregor, 1931; Phillips, 1959, 1961; and Almond, 1964), but ultramafic rocks from high-grade contact-metamorphic environments contain spinel rather than plagioclase (Matthes, 1971).

This report describes the occurrence of hornblende–plagioclase peridotite hornfels in the contact

[1] Present address: Department of Geology, University of Minnesota–Duluth, Duluth, Minnesota 55812.

zone of a gabbro, where it has formed in aluminous zones in an enstatite and chromite-bearing metaperidotite. The relationships displayed permit refinement of the low-temperature and high-pressure limits to the stability of plagioclase in peridotite, and provide an explanation for the rarity of plagioclase in metamorphosed ultramafics.

Location and regional geology

The hornblende–plagioclase peridotite occurs in a metamorphosed ultramafic complex on the north slope of the Icicle Creek valley in the central Cascades of Washington, about 115 km east of Seattle (Fig. 1). It is a part of the Mount Stuart block, a fault-bound structural unit which comprises the Mount Stuart Batholith and the rocks it has intruded and metamorphosed. These country rocks include the Chiwaukum Schist, a pelitic schist that is the southern continuation of the Skagit Metamorphic Suite (Misch, 1966), and the Ingalls Complex, a tectonically emplaced ultramafic-mafic complex.

The Chiwaukum Schist underwent an early Barrovian-type regional metamorphism of unknown age, which reached the staurolite grade in the Icicle Creek area. The Ingalls Complex was emplaced after this regional metamorphism, and the associated deformation jumbled the units so that inclusions of diabasic to gabbroic rock, and less commonly, Chiwaukum Schist, chert, and felsic plutonic rock occur locally within the ultramafic units. Concurrent with the emplacement, or somewhat afterward, the complex underwent a low-grade hydrothermal event which serpentinized large portions of the peridotite.

The Mount Stuart Batholith is of Late Cretaceous age and is composed of two major phases, an earlier mafic phase which ranges from gabbro to diorite and a later silicic phase which ranges from quartz–diorite to granodiorite (Pongsapich, 1974). Intrusion of the batholith resulted in contact metamorphism of both the Chiwaukum Schist and the Ingalls Complex. In the aureole of the silicic phase of the batholith, staurolite, cordierite, and andalusite crystallized or recrystallized in the schist, while in the aureole of the mafic phase, sillimanite grew as well (Plummer, 1969). Contact metamorphism of the Ingalls Complex by the silicic phase of the batholith at Paddy-Go-Easy Pass, about 23 km southeast of the Icicle Creek area, caused the formation of the forsterite–enstatite–tremolite assemblage in the metaperidotite and the forsterite–enstatite–spinel assemblage in associated aluminous metamorphosed blackwall rocks (Frost, 1975).

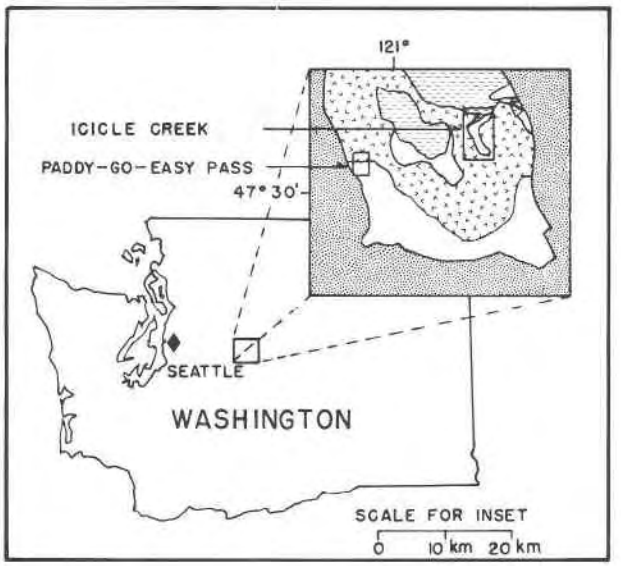

FIG. 1. Map showing location of areas in the central Cascades of Washington where contact metamorphism of peridotite and related rocks has been studied; Icicle Creek, this paper, Paddy-Go-Easy Pass, Frost (1975). Dashed symbols = Chiwaukum Schist, blank = Ingalls Mafic-Ultramafic Complex, v-symbols = Mount Stuart Batholith, dotted symbols = Tertiary sedimentary rocks.

Petrographic description

In the Icicle Creek area the Ingalls Complex survives as two bodies which cover a total area of about 8 km² adjacent to and within the mafic phase of the Mount Stuart Batholith (Fig. 2). Throughout these bodies the metaperidotite contains the assemblage forsterite–enstatite–tremolite–chlorite, even in localities more than a kilometer from the nearest contact (Pongsapich, 1974). In the larger body the associated mafic inclusions within the metaperidotite are typical hornblende hornfelses, but in a small pendant in the batholith (Fig. 2), the mafic hornfelses locally develop the assemblage hornblende–orthopyroxene–clinopyroxene–plagioclase (An60). A pelitic hornfels with the assemblage biotite–plagioclase (An40)–cordierite–hypersthene also occurs within the pendant.

Wherever the mafic hornfels and metaperidotite are in contact, a mineralogically and chemically complex metasomatic reaction zone has developed between them. There seem to be two different types of reaction zones (Fig. 3), a two-part reaction zone, and an amphibole-rich one. The more common two-part reaction zone is similar to that described from Paddy-Go-Easy Pass (Frost, 1975), where an aluminous "blackwall" zone and a calcic "metarodingite" zone surround the mafic inclusion. The amphibole-rich reaction zone, in which hornblende or tremolite make

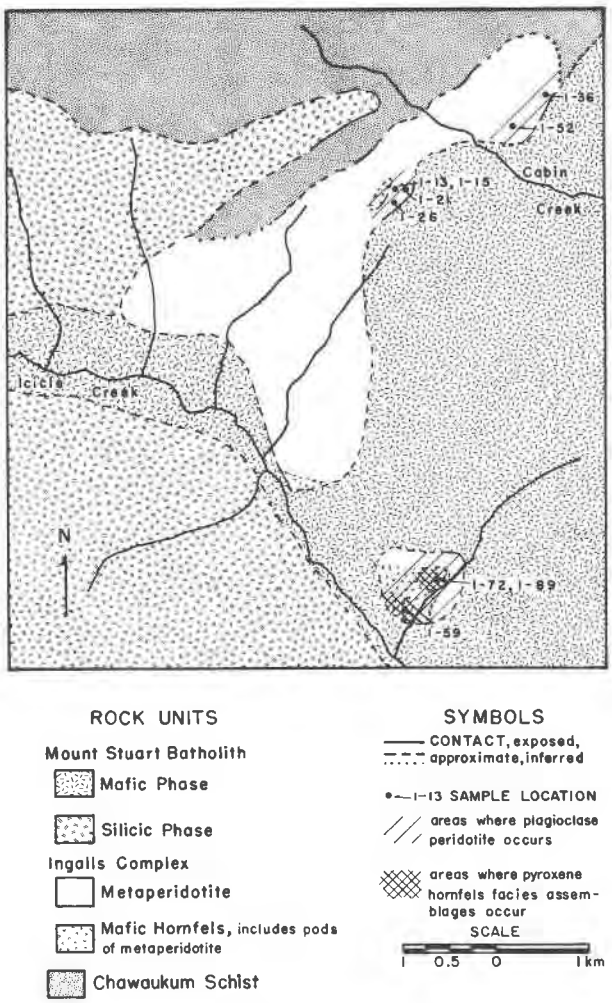

FIG. 2. Geologic map of the Icicle Creek area, Washington. Geologic mapping by Pongsapich (1974) with revisions by Frost. Topographic base from U.S. Geological Survey 15 minute Chiwaukum Mountains quadrangle.

up more than 75 percent of the rock and spinel is absent, seems to show a transition from tremolite-rich metaperidotite, through a rock rich in an amphibole which is colorless in thin section, through hornblendite, where the amphibole is brown or olive-colored, to mafic hornfels.

The hornblende–plagioclase peridotites occur as part of the aluminous reaction zones within several hundred meters of the contact with the mafic phase of the batholith. They are orange or green on a weathered surface and cinnamon-brown to dark-green when fresh. Modal proportions of the constituent phases are quite variable. For example, colorless or very pale brown or green hornblende makes up between 5 and 40 percent of a rock. Generally it is embayed by the other phases and contains numerous inclusions of green spinel. Anhedral, rounded olivine makes up 30 to 40 percent of the hornblende–plagioclase peridotites, and irregularly shaped, spongy enstatite occurs in amounts between 0 and 20 percent. Anorthitic plagioclase (An 98–99) makes up 20 to 25 percent of the rock, forming large, irregular grains, commonly rimming spinel. Brown to green spinel is usually quite abundant, forming up to 20 percent of some rocks. Most of the rocks have a granoblastic texture, and many of them are banded with layers richer in olivine and plagioclase alternating with those containing more hornblende and spinel.

Mineral compositions

In order to understand how the mineral compositions affect the phase equilibria, constituent minerals from five samples of hornblende–plagioclase peridotite, two samples of enstatite- and diopside-bearing tremolite hornfels, and one sample each of forsterite–enstatite–tremolite metaperidotite, hornblende-bearing pyroxene hornfels, and cordierite–hypersthene hornfels were analyzed on an Applied Research Laboratories 5-channel EMX-SM microprobe (Table 1). The sample locations are shown on Figure 2.

Individual grains of olivine, enstatite, and diopside were of uniform composition for all samples studied. However, there was grain-to-grain variation ranging from moderate to extreme, especially in rocks from the reaction zones. In order to minimize the effect of this variation, analyses reported from a particular sample were taken from neighboring grains within a circle 0.5 cm in diameter. Spinel, plagioclase, and hornblende, although uniform in composition in some samples, showed within-grain zoning as well as grain-to-grain variation. Unless otherwise indicated, analyses are average values.

Olivine and orthopyroxene

The olivine and orthopyroxene from the Icicle Creek rocks show similar composition ranges to those from Paddy-Go-Easy Pass (Frost, 1975), namely Fo_{90},En_{91} in the metaperidotite and Fo_{79-89}, En_{80-90} in the aluminous reaction zone rocks (Tables 2, 3). Orthopyroxene richer in iron (En_{68},En_{48}) occurs in the hornblende–pyroxene and biotite–cordierite–hypersthene hornfelses, respectively. As at Paddy-Go-Easy Pass, clinoenstatite lamellae in orthoenstatite occur locally throughout the area. Undulose extinction along with minor bending and kink-

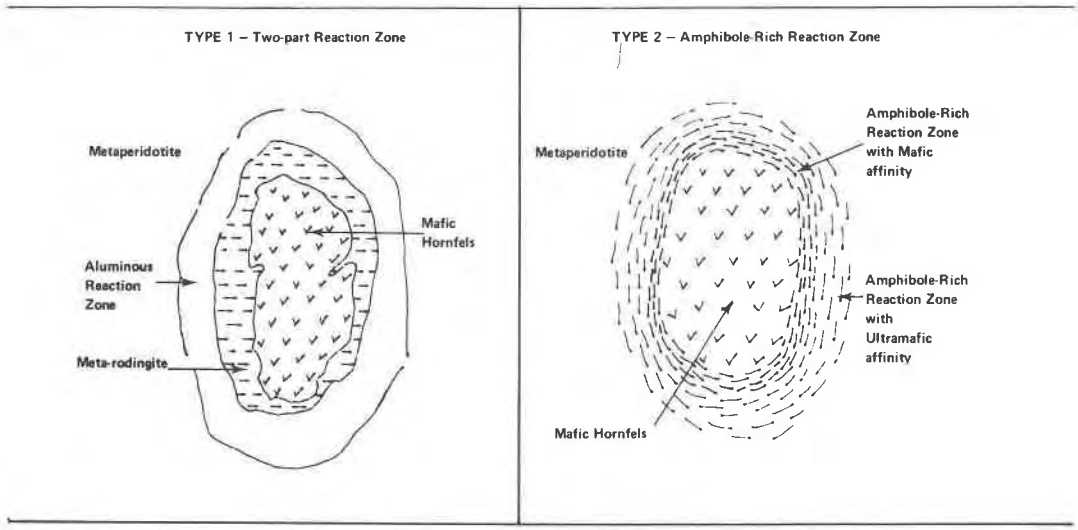

ASSEMBLAGES ENCOUNTERED

Metaperidotite	Aluminous R.Z.	Metarodingite	Amphibole-rich Ultramafic affinity	Amphibole-rich Mafic affinity	Mafic Hornfels
Ol-Opx-Tr-Cte-Chromite	(Plag = An_{98-99})	(Plag = An_{90-96})	(Amphibole=colorless colorless hornblende)	(Amphibole=brown-olive hornblende)	(Amphibole=brown hornblende)
	Hb-Ol-Sp	Cpx-Plag	Hb	(Plag ioclase=An_{70-80})	(Plagioclase=An_{65-70})
	Hb-Ol-Opx-Sp	Cpx-Plag-Garn	Hb-Opx		
	Ol-Plag-Hb-Sp	Cpx-Plag-Sp	Hb-Opx-Ol	Hb-Plag	Hb-Plag
	Ol-Opx-Hb-Plag	Cpx-Sp	Hb-Cpx-Opx-Chromite*	Hb-Di-Plag	Hb-Plag-Di
	Ol-Opx-Hb-Plag-Sp			Hb-Ol-Plag	Hb-Plag-Opx
	Ol-Opx-Plag-Sp			Hb-En-Di-Plag*	Hb-Plag-Opx-Cpx*
	Ol-Hb-Di-Sp				

* Assemblages transitional to pyroxene-hornfels facies

Cpx=clinopyroxene, Cte=chlorite, Garn=garnet, Hb=hornblende, Ol=olivine, Opx=orthopyroxene, Plag=plagioclase, Sp=spinel, Tr= tremolite.

FIG. 3. Diagramatic display of the two types of reaction zones found around mafic inclusions in the metaperidotite. The mineral assemblages listed are those encountered in the highest-grade areas, indicated by ruled lines in Fig. 2. Width of the reaction zones is variable, ranging from 10 to 50 centimeters.

ing of the orthoenstatite indicate that the clinoenstatite is strain-induced.

Al_2O_3 content of the orthopyroxene ranges from less than 1.0 percent for those pyroxenes from rocks not containing highly aluminous phases, to 3.7 percent for the hypersthene coexisting with cordierite. The orthopyroxene occurring with green spinel and olivine contains only about 3.2 percent Al_2O_3, somewhat less than one would expect from the experimental work of MacGregor (1974).

TABLE 1. List of analyzed rock samples from Icicle Creek

I-13	Hornblende-Plagioclase Peridotite
I-15	Hornblende-Plagioclase Peridotite
I-21	Hornblende-Plagioclase Peridotite
I-26	Hornblende-Plagioclase Peridotite
I-36	Metaperidotite, Forsterite-Enstatite-Tremolite Assemblage
I-52a	Reaction-zone rock with mafic affinities, Forsterite-Anorthite-Spinel Assemblage
I-52b	Reaction-zone rock with mafic affinities, Hornblende-Ortho-pyroxene-Clinopyroxene-Labradorite Assemblage
I-59	Hornblende-Pyroxene Hornfels
I-72	Tremolite-Enstatite-Diopside-Chromite Hornfels
I-82	Tremolite-Enstatite-Diopside-Chromite Hornfels
I-89	Cordierite-Hypersthene Hornfels

Distribution of Fe and Mg between olivine and enstatite (Fig. 4) shows a $K_d = 0.9$, consistent with other pairs from ultramafic rocks (Ross *et al.*, 1954; Green, 1964; Challis, 1965; White, 1966; Peters, 1968; Loney *et. al.*, 1971; Medaris, 1972; Onyeagocha, 1973; Evans and Trommsdorff, 1974; and Frost, 1975).

Clinopyroxene

Clinopyroxene from all of the rocks is strongly magnesian, and even that from the hornblende–pyroxene hornfels has an X_{Mg} greater than 0.80. Al_2O_3 and Na_2O contents are low, less than 2.00

TABLE 2. Microprobe analyses of olivine

	I-36	I-15	I-21	I-13	I-26	I-52a
SiO_2	40.56	39.57	40.27	38.45	40.08	38.80
FeO*	9.17	14.30	10.24	18.20	11.30	18.52
MgO	49.45	45.29	48.32	41.81	47.51	41.55
MnO	0.16	0.28	0.07	0.39	0.16	0.27
NiO	0.25	0.04	0.08	0.32	0.27	0.24
CaO	0.02	0.03	0.04	0.06	0.04	ND
Total	99.62	99.50	99.02	99.22	99.36	99.38
	Cation Proportion on a basis of 4 oxygens					
Si	0.996	0.996	0.999	0.992	0.997	0.998
Fe	0.188	0.301	0.212	0.392	0.235	0.398
Mg	1.810	1.699	1.786	1.607	1.762	1.595
Mn	0.003	0.006	0.002	0.008	0.003	0.006
Ni	0.005	0.001	0.002	0.007	0.006	0.005
Ca	0.001	0.001	0.001	0.002	0.001	ND
Mg/Fe + Mg	0.906	0.850	0.894	0.804	0.882	0.800

* Total iron as FeO. ND = not determined.

and 0.30 percent, respectively, values which are undoubtedly an indication of the low-pressure and relatively low-temperature origin of these rocks.

Distribution of Fe and Mg between the pyroxenes defines a $K_d = 0.60$ (Fig. 4). This is lower than the K_d of between 1.00 and 0.7 found in other ortho–clinopyroxene pairs (Ross *et. al.*, 1954; Kretz, 1961; White, 1966; Peters, 1968; Medaris, 1972; and Onyeagocha, 1973). Apart from the obvious temperature effect, this difference is also related to the fact that the lower-temperature diopside from Icicle Creek is more calcic than diopside from the higher-temperature rocks. As pointed out by Blander (1972), iron content of clinopyroxene is dependent upon the extent to which the *M*2 site is occupied by calcium.

The ortho–clinopyroxene pairs from Icicle Creek define a solvus which is considerably wider than that determined at 810°C by Lindsley *et al.* (1974) (Fig. 5). Other pyroxene geothermometers also yield unreasonably high temperatures for these pairs, *ca.* 900°C for the equations of Wood and Banno (1973) and *ca.* 1000°C for those of Saxena and Nehru (1975). This discrepancy is undoubtedly due to the fact that their equations were derived by extrapolation from high-temperature experiments. As a result, they are probably not valid for these relatively low-temperature rocks. Furthermore, Saxena and Nehru

TABLE 3. Microprobe analyses of pyroxenes

	I-36	I-26	I-21	I-52b*	I-52b**	I-59*	I-59**	I-72*	I-72**	I-89
SiO_2	57.09	56.06	55.51	55.53	53.07	53.97	52.95	57.43	54.77	49.23
TiO_2	0.00	0.06	0.13	0.07	0.14	0.11	0.23	0.00	0.01	0.12
Al_2O_3	1.21	1.87	3.16	1.68	1.90	0.95	1.28	0.46	0.51	3.49
Cr_2O_3	0.13	0.07	0.00	0.02	0.11	0.03	0.06	0.07	0.15	0.06
FeO***	5.74	7.16	6.70	12.62	4.73	18.89	6.54	9.36	2.79	30.01
MgO	35.42	33.69	33.58	28.96	16.48	24.10	15.25	32.13	17.81	15.72
CaO	0.18	0.32	0.22	0.50	22.86	0.61	22.75	0.59	23.61	0.24
MnO	0.16	0.15	0.08	0.29	0.16	0.99	0.45	0.20	0.11	0.46
NiO	0.06	0.08	0.03	0.04	0.03	0.02	0.02	0.06	0.05	0.00
Na_2O	0.00	0.00	0.00	0.00	0.23	0.00	0.29	0.01	0.19	0.00
Total	99.99	99.46	99.42	99.72	99.70	99.67	99.81	100.22	99.97	99.33
	Cation proportions on a basis of 6 oxygens									
Si	1.964	1.952	1.927	1.975	1.951	1.986	1.963	2.000	1.990	1.917
Al IV	0.036	0.048	0.073	0.025	0.049	0.014	0.037	0.000	0.010	0.083
Al VI	0.012	0.028	0.057	0.045	0.033	0.027	0.019	0.019	0.012	0.077
Ti	0.000	0.002	0.003	0.002	0.004	0.003	0.006	0.000	0.000	0.004
Cr	0.004	0.002	0.000	0.000	0.003	0.001	0.002	0.002	0.004	0.002
Fe	0.165	0.209	0.195	0.375	0.145	0.581	0.203	0.273	0.085	0.977
Mg	1.816	1.749	1.738	1.535	0.903	1.322	0.843	1.668	0.965	0.913
Ca	0.007	0.012	0.008	0.019	0.900	0.024	0.904	0.018	0.919	0.010
Mn	0.005	0.004	0.002	0.009	0.005	0.030	0.014	0.006	0.003	0.015
Ni	0.002	0.002	0.000	0.001	0.001	0.001	0.000	0.002	0.001	0.000
Na	0.000	0.000	0.000	0.000	0.017	0.000	0.021	0.000	0.012	0.000
Sum VI ions	2.011	2.008	2.003	1.986	2.011	1.998	2.012	1.988	2.001	1.998
Wo	0.34	0.60	0.43	0.99	46.20	1.25	46.36	0.95	46.69	0.53
En	91.36	88.80	89.55	79.56	46.34	68.58	43.23	85.13	49.00	48.03
Fs	8.30	10.59	10.03	19.45	7.46	30.17	10.41	13.92	4.30	51.44

* Orthopyroxene from orthopyroxene-clinopyroxene pair.
** Clinopyroxene from orthopyroxene-clinopyroxene pair.
*** Total iron as FeO.

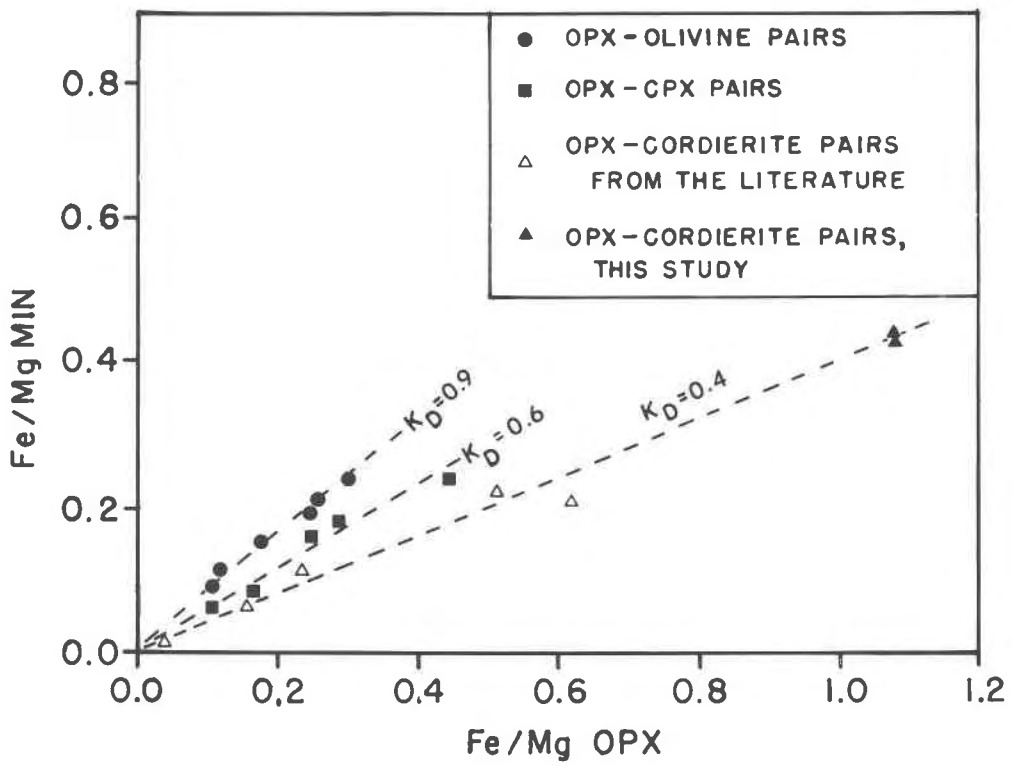

FIG. 4. Distribution of iron and magnesium between orthopyroxene and coexisting olivine, clinopyroxene, and cordierite. Analyses quoted from the literature are those of Barker (1964), Chinner and Sweatman (1968), Reinhardt (1968), and Knorring *et al.* (1969).

(1975) have derived their geothermometer using a series of complex expressions indicating the amount of the various ions in the $M1$ and $M2$ sites. Since the site preferences are very poorly known, particularly in the clinopyroxenes, and since they are surely a function of temperature, if not of composition, this geothermometer can hardly be applied rigorously to low-temperature pyroxene pairs.

Spinel

Spinel ranges in composition from green, aluminous spinel in the hornblende–plagioclase peridotite to chromite with more than 60 percent $(Fe,Mg)Cr_2O_4$ in the tremolite–enstatite–diopside hornfels (Table 5). Three of the samples (I-15, I-21, and I-52) contain green spinel which is unzoned and shows only minor grain-to-grain variation. The remaining samples contain weakly-zoned spinels with a rather sizable grain-to-grain variation. The iron and magnesium distribution between olivine and spinel is dependant upon the chrome content of the spinel and shows a similar trend to that described by Evans and Frost (1975) (Fig. 6).

Cordierite

Cordierite from the pelitic hornfelses is fairly iron-rich and may contain about 3 weight percent H_2O, as determined by totals of 97 percent from microprobe analysis (Table 5). This value is within the range of 0.32–4.8 percent found in wet-chemical analyses of cordierite tabulated by Leake (1960). The K_d for iron and magnesium distribution between cordierite and hypersthene from Icicle Creek is consistent with that from other cordierite–hypersthene pairs (Barker, 1964; Chinner and Sweatman, 1968; Reinhardt, 1968; and Knorring *et al.*, 1969) (Fig. 4). These mineral pairs came from rocks which formed under a wide variety of P-T environments, and the cordierite in them contains differing amounts of H_2O (ranging from 0.3 to 3.0 percent), indicating that the water content of cordierite may not have as strong an affect on the K_d between cordierite and other ferromagnesian phases as has been postulated (Wood, 1973).

Calcic amphiboles

The calcic amphiboles from the Icicle Creek rocks range in composition from tremolite to hornblende

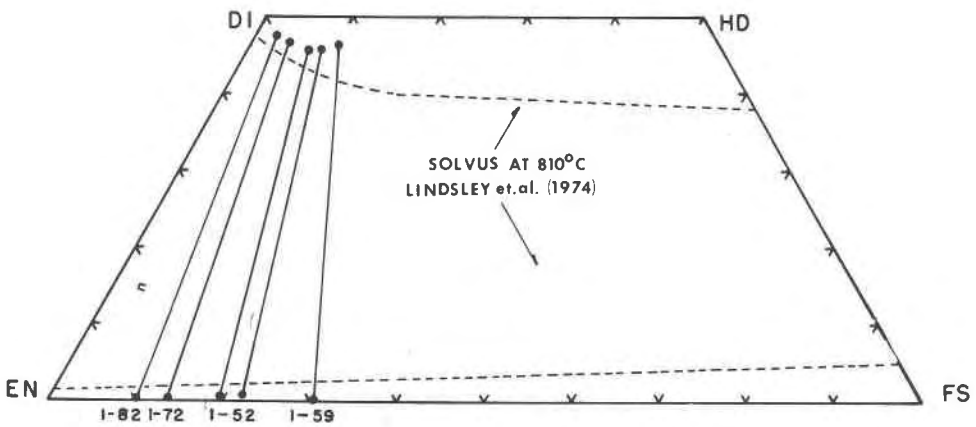

FIG. 5. Solvus defined by coexisting orthopyroxene and clinopyroxene as compared with that determined experimentally by Lindsley *et al.* (1974).

(Table 6), with two different trends in amphibole composition (Fig. 7). Hornblende from the hornblende–plagioclase peridotite, which is colorless in thin section and occurs with olivine, enstatite, anorthite, and spinel, shows a trend toward a hornblende rich in the tschermakite end member, with a (Na + K)/Al^{IV} ratio of 0.15. This trend is different from that described by Frost (1975) from forsterite–enstatite–spinel rocks, but is similar to the (Na + K)/Al^{IV} values from highly tschermakitic amphiboles reported by Leake (1971).

The brown hornblende from the mafic hornfels, where it occurs with clinopyroxene, orthopyroxene, and labradorite, and the tremolite from the tremolite–enstatite–diopside–chromite rocks are relatively more sodic, showing a (Na + K)/Al^{IV} trend more in the direction of pargasite. The colored hornblende of the mafic rocks further differs from the colorless hornblende of the ultramafic rocks in that it contains more iron, apparently as Fe^{2+}, more titanium relative to aluminum, and according to calculations of Papike *et al.* (1974), has minor amounts of sodium in the *M*4 site.

TABLE 4. Microprobe analyses of plagioclase

	I-21	I-26	I-59
SiO_2	43.16	43.45	52.85
Al_2O_3	36.32	36.50	30.04
Fe_2O_3*	0.06	0.13	0.23
CaO	19.87	20.15	12.47
MgO	0.00	0.01	0.03
Na_2O	0.17	0.09	4.43
K_2O	0.00	0.00	0.12
Sum	99.58	100.32	100.17
Cation proportion on a basis of 8 oxygens			
Si	2.007	2.007	2.392
Al	1.991	1.987	1.603
Fe^{+3}	0.002	0.004	0.008
Ca	0.990	0.997	0.605
Mg	0.000	0.000	0.002
Na	0.016	0.008	0.389
K	0.000	0.000	0.007
Total	8.000	8.000	8.000
An	99.4	99.2	60.5

* Total iron as Fe_2O_3.

The solid line in Figure 7 reflects the manner in which the amphibole composition is controlled by that of the coexisting phases. From the slope of this line the hornblende composition in the hornblende–plagioclase peridotites can be approximated by the formula

$$Na_{0.15x}Ca_2Mg_{5-0.85x}(Si_{8-x}Al_xO_{22})(OH)_2$$

This hornblende coexists with olivine, enstatite, and spinel; therefore, its composition is fixed by the reaction:

$$\text{tremolite} + 0.925x \text{ spinel} + 0.075x Na_2O = \text{hornblende } (Al^{IV} = x) + 0.775x \text{ forsterite} + 0.225x \text{ enstatite} \quad (1)$$

Assuming that the Na_2O is in the fluid phase, this reaction involves six components and five phases, and, therefore, is isothermally and isobaricly univariant. The univariant nature of this reaction is expressed as the linear relationship in Figure 7. Why the hornblende from olivine, enstatite, and spinel-bearing assemblages from Paddy-Go-Easy Pass has a different value of (Na + K)/Al^{IV} from that at Icicle

TABLE 5. Microprobe analyses of spinel and cordierite

	I-15	I-21	I-26*	I-27*	I-36	I-72**	I-89***
SiO_2	ND	ND	ND	ND	ND	ND	48.81
TiO_2	0.02	0.03	0.08	0.00	0.05	0.02	0.00
Al_2O_3	66.1	67.0	35.7	27.4	21.1	15.3	31.52
Cr_2O_3	0.04	0.05	27.3	32.2	43.0	50.0	0.00
Fe_2O_3	1.55	0.85	5.64	7.42	4.60	3.33	—
V_2O_3	0.16	0.07	0.09	0.06	0.35	0.05	ND
MgO	19.7	21.2	12.4	6.88	9.24	7.13	9.07
FeO	12.1	9.62	18.2	29.2	20.2	22.7	7.22☆
MnO	0.12	0.03	0.11	0.21	0.45	0.17	0.12
NiO	0.02	0.12	0.21	0.07	0.04	0.03	0.00
ZnO	0.11	0.12	0.17	0.21	0.37	0.40	ND
Total	99.92	99.09	99.90	99.65	99.40	99.13	96.88
	Cation proportions on a basis of 32 oxygens						
Si	ND	ND	ND	ND	ND	MD	5.074☆☆
Ti	0.003	0.005	0.014	0.000	0.010	0.004	0.000
Al	15.726	15.852	9.891	8.158	6.348	4.788	3.863
Cr	0.006	0.008	5.066	6.421	8.678	10.527	0.000
Fe+3☆☆☆	0.236	0.129	0.998	1.408	0.882	0.666	—
V	0.026	0.011	0.017	0.012	0.072	0.011	ND
Mg	5.927	6.343	4.341	2.587	3.516	2.828	1.405
Fe	2.036	1.614	3.581	5.315	4.319	5.053	0.628
Mn	0.021	0.005	0.022	0.045	0.097	0.038	0.010
Ni	0.003	0.019	0.040	0.014	0.008	0.006	0.000
Zn	0.016	0.018	0.030	0.039	0.070	0.079	0.000
Y_{Al}	0.985	0.992	0.620	0.510	0.399	0.300	—
Y_{Cr}	0.000	0.000	0.318	0.402	0.546	0.659	—
Mg/Fe+Mg	0.744	0.797	0.548	0.327	0.449	0.359	0.691

* Value represents an average of the six most chromiferous points.
** Value represents an average of the six most aluminous points.
*** Analysis of cordierite, includes 0.05% CaO and 0.08% Na_2O.
☆ Total iron as FeO.
☆☆ Cation proportions for cordierite calculated on a basis of 18 oxygens.
☆☆☆ Fe_2O_3 for spinel calculated assuming stoichiometry.
ND = Not determined.

Creek is not understood, but it could be related to different external parameters between the two aureoles.

The hornblende in the hornblende–plagioclase peridotite generally contains more sodium than coexisting plagioclase. For reasons of charge balance, the substitution of sodium into plagioclase is accompanied by addition of silica and expulsion of aluminum, whereas the substitution of sodium into hornblende requires the *addition* of aluminum and the removal of silica from the amphibole. As the hornblende–plagioclase peridotite contains olivine and spinel and is relatively saturated in aluminum and undersaturated in silica, the admission of sodium into the amphibole is obviously favored.

Estimate of pressure and temperature at the time of metamorphism

The pelitic minerals in the contact aureole indicate a relatively low pressure of metamorphism. Plummer

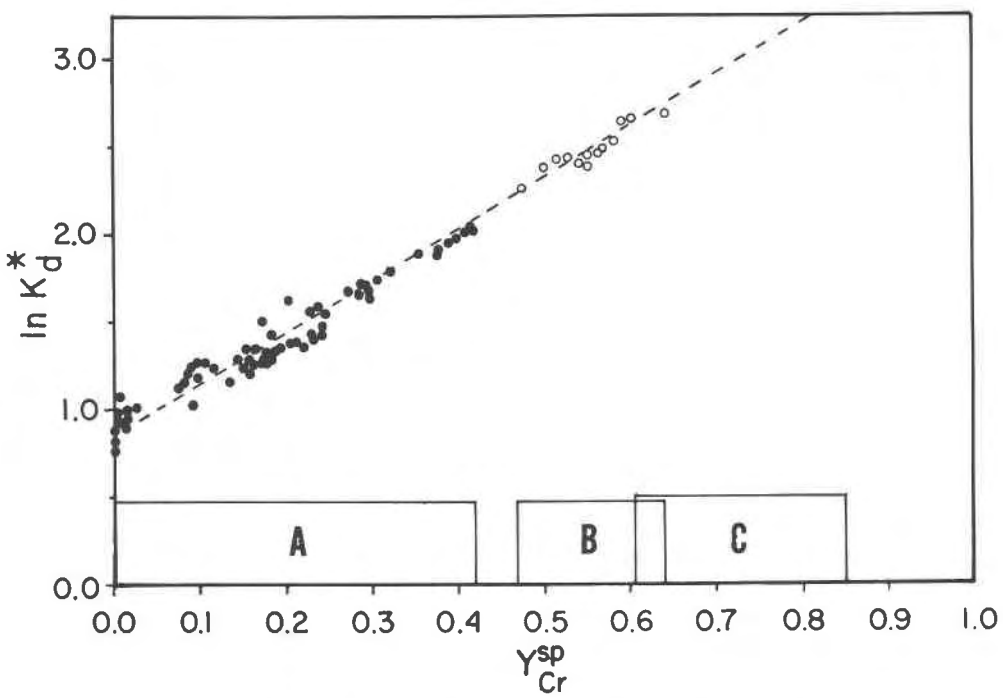

FIG. 6. Logarithm of the partition coefficient for the distribution of iron and magnesium between olivine and spinel as a function of Y_{Cr}^{sp} (where Y_{Cr}^{sp} = Cr/Al + Cr + Fe^{3+}), calculated assuming that $Y_{Fe}^{sp}3+ = 0.05$ (ln K_d = ln K_d + 4(0.05 − $Y_{Fe}3+)^{sp}$. The dashed line is the ca. 700°C "isotherm" of Evans and Frost (1975). *A* = composition range of spinel from the hornblende–plagioclase peridotite, solid circles, *B* = composition range of spinel from metaperidotite, open circles, *C* = composition range of spinel from tremolite–enstatite–diopside–chromite assemblage.

(1969) noted that staurolite seemed to be stable with both cordierite and andalusite within the aureole. The presence of staurolite would place the low-pressure limit at about 2 kilobars (Richardson, 1968) and the occurrence of the other minerals would suggest pressures of between 2.5 and 4 kilobars (Hess, 1969). The lack of cordierite as a breakdown product of chlorite is not inconsistent with these estimated pressures, for as noted by Frost (1975) the presence of minor elements, most notably iron and chromium, and the occurrence of unknown amounts of water in the cordierite, lower the upper pressure limit for the reaction forsterite + cordierite = enstatite + spinel to pressures much lower than the 3.3 kilobars (730°C) found in the pure system (Fawcett and Yoder, 1966).

Although P_{H_2O} is unknown, its maximum value can be safely set at P_{total}. This is particularly true in the metaperidotite where progressive metamorphism would have continually enriched the fluid phase in H_2O. The same may not be true for the mafic hornfelses, because when epidote (which is only a minor phase to begin with) reacts out at relatively low temperatures, there are no major dehydration reactions until the breakdown of hornblende. Lower P_{H_2O} in the mafic inclusions relative to the metaperidotite is indicated by the fact that the only rocks containing assemblages in the pyroxene–hornfels facies (*i.e.* orthopyroxene + clinopyroxene in either the mafic or ultramafic hornfelses) are found associated with the larger mafic inclusions in the roof pendant. This localization does not seem to be due to variations in rock composition, as in one locality an ultramafic, tremolite-rich rock included in mafic hornfels contains the assemblage enstatite–diopside–tremolite, indicating that the reaction forsterite + tremolite = enstatite + diopside + H_2O has gone to completion with the elimination of olivine from the rock. The metaperidotite elsewhere in the roof pendant still contains the assemblage forsterite + tremolite. This suggests that the rocks containing the pyroxene–hornfels facies assemblages formed in areas of relatively low P_{H_2O} where hornblende had become unstable, while throughout the metaperidotite P_{H_2O} was great enough to maintain amphibole as a stable phase.

The breakdown of chlorite occurs in the metape-

ridotite near the contact with the batholith, allowing a temperature estimate to be obtained from the experimentally determined curve for the reaction chlorite = forsterite + enstatite + spinel + H_2O. By setting the pressure limits at 2 and 4 kilobars and taking into account iron substitution (Frost, 1975), then the temperature limits can be calculated from the equation:

$$\ln f_{H_2O} = -7620/T + 7.59 + 0.1856(P - 3000)/T \text{ (Frost, 1975)}$$

The resulting temperatures are 690° and 740° for pressures of 2 and 4 kilobars, respectively. Although this result (715 ± 25°C) is subject to error inherent in the determination of the equilibrium expression (Frost, 1975), this error will have only a minor effect on the conclusions.

Topologies for phase equilibria governing the occurrence of plagioclase in metaperidotite

Phase relations in aluminous peridotite can be approximated by the $CaO–MgO–Al_2O_3–SiO_2–H_2O$ system. As no plagioclase has been found in metaperidotite occurring below the anthophyllite-out isograd (Frost, 1975), low-temperature Mg-silicates antigorite, talc, and anthophyllite can be disregarded. The participating phases are therefore limited to anorthite, chlorite, diopside, enstatite, forsterite, spinel, calcic amphibole, and water. The composition of chlorite is taken to be $Mg_5Al_2Si_3O_{10}(OH)_8$, as that is close to the composition of chlorite found at its breakdown in high-grade metamorphosed blackwall rocks (Frost, 1975).

A Schreinemakers' analysis of this system using the phases listed, after the method of Zen (1966), yields 8

TABLE 6. Microprobe analyses of calcic amphiboles

	I-15	I-21	I-26	I-13	I-26*	I-26**	I-72	I-59
SiO_2	46.08	46.46	50.46	46.30	42.63	42.50	55.74	47.88
TiO_2	1.59	1.73	0.28	1.06	0.97	3.02	0.01	1.66
Al_2O_3	13.23	12.70	9.20	11.65	14.59	12.24	3.08	8.39
Cr_2O_3	0.02	0.00	0.39	0.59	0.07	0.38	0.33	0.16
FeO***	4.86	3.91	4.03	5.99	7.75	8.30	3.57	10.01
MgO	17.24	18.13	19.74	17.41	15.76	15.59	22.32	15.80
MnO	0.12	0.04	0.05	0.12	0.10	0.10	0.05	0.27
NiO	0.00	0.03	0.08	0.07	0.06	0.07	0.11	0.02
CaO	12.24	12.32	12.45	11.91	11.73	11.63	11.72	11.16
Na_2O	0.36	0.22	0.48	0.10	2.47	2.68	0.51	1.28
K_2O	0.81	1.01	0.09	1.40	0.39	0.64	0.15	0.43
Total	96.54	96.55	97.26	96.59	96.51	97.14	97.59	97.07
			Cation proportion on a basis of 23 oxygens					
Si	6.550	6.581	7.041	6.640	6.209	6.210	7.682	6.928
Al_{IV}	1.450	1.419	0.959	1.360	1.791	1.790	0.318	1.072
Al_{VI}	0.723	0.702	0.554	0.611	0.715	0.318	0.182	0.360
Ti	0.167	0.184	0.029	0.115	0.106	0.332	0.001	0.181
Cr	0.002	0.000	0.043	0.067	0.088	0.044	0.036	0.018
Fe	0.578	0.463	0.470	0.718	0.944	1.014	0.412	1.212
Mg	3.653	3.827	4.106	3.771	3.420	3.394	4.586	3.408
Mn	0.014	0.004	0.005	0.014	0.012	0.012	0.006	0.331
Ni	0.000	0.003	0.010	0.009	0.007	0.008	0.012	0.003
Ca	1.865	1.869	1.862	1.830	1.830	1.820	1.731	1.730
Na	0.100	0.060	0.130	0.027	0.699	0.758	0.137	0.360
K	0.146	0.183	0.015	0.256	0.072	0.120	0.026	0.078
$Na+K/Al^{IV}$	0.170	0.174	0.151	0.208	0.430	0.490	0.513	0.408

* Margin of zoned hornblende grain, colorless in PPL
** Core of zones hornblende grain, brown in PPL
*** Total iron as FeO.

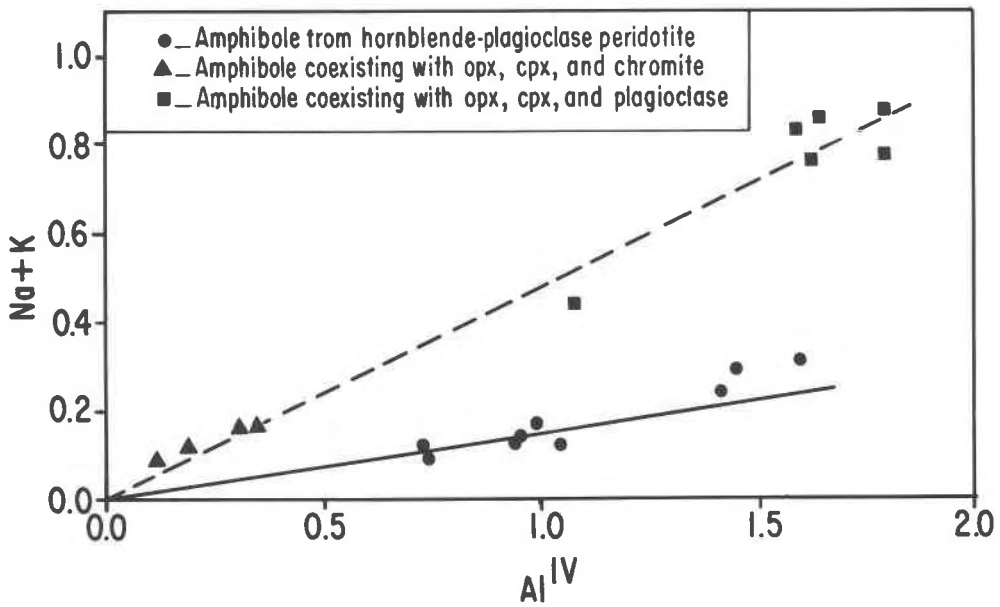

FIG. 7. Variations of the alkali content of amphiboles as a function of tetrahedral aluminum, calculated on an anhydrous basis of 23 oxygens.

invariant points which are connected by 32 univariant curves. Fortunately the relative positions of three of the univariant curves are known. Experimental work cited above (*e.g.* Kushiro and Yoder, 1966) places the reaction forsterite + anorthite = enstatite + diopside + spinel at relatively high pressure (6–10 kbar) with a relatively small value of dP/dT. Field evidence indicates that the reaction chlorite = forsterite + enstatite + spinel + H_2O occurs at lower temperatures than the reaction forsterite + tremolite = enstatite + diopside + H_2O for most metamorphic pressure conditions (Trommsdorff and Evans, 1974; Frost, 1975). This enables one to construct a unique topologic net for equilibria involving these phases (Frost, 1973, Fig. 48). Comparison of the assemblages found in the metarodingite and metamorphosed blackwall rocks at Paddy-Go-Easy Pass with those predicted by the topologic net indicates that the plagioclase-producing reactions occur at temperatures and pressures above those of the invariant point produced by the intersection of the reactions chlorite = forsterite + enstatite + spinel + H_2O and tremolite + diopside + spinel = anorthite + forsterite + H_2O. This allows one to further reduce the significant reactions to those shown on Figure 8 (Frost, 1973). The stoichiometry of these reactions is given in Table 7.

Chemographic diagrams projected from forsterite to the CaO–Al_2O_3–SiO_2 plane of the MgO–CaO–Al_2O_3–SiO_2 tetrahedron show that most of the assemblages encountered in the Icicle Creek rocks are consistent with the theoretically derived phase diagram (Fig. 8). Two rock samples, however, contain the assemblage tremolite–diopside–enstatite–chromite, which is diagnostic of the "higher pressure" divariant field bounded by reactions (An,Sp) and (Fo). The Icicle Creek hornfelses, though, may be assumed to have formed under isobaric conditions. In the next section it is shown that the reaction (V, Tr) and hence the whole diagram (Fig. 8) is translated to lower pressures by impurities such as Fe^{2+}, Fe^{3+}, and Cr in the participating phases.

Effect of impurities on the reaction forsterite + anorthite = enstatite + diopside + spinel

The effect of other components (*e.g.* chromium, iron), particularly in spinel, on the H_2O-absent reaction can be estimated by simple thermodynamics, and this result can be compared with the estimates for temperature and pressure derived independently for the Icicle Creek rocks. The equilibrium is:

$$\underset{\text{forsterite}}{2Mg_2SiO_4} + \underset{\text{anorthite}}{CaAl_2Si_2O_8} = \underset{\text{enstatite}}{Mg_2Si_2O_6} + \underset{\text{diopside}}{CaMgSi_2O_6} + \underset{\text{spinel}}{MgAl_2O_4}$$

and,

$$K = \frac{(a_{en}^{opx})(a_{di}^{cpx})(a_{MgAl_2O_4}^{sp})}{(a_{fo}^{ol})^2(a_{an}^{plag})}$$

For minor amounts of dilution, Raoult's law can be assumed to hold approximately, and therefore for spinel and olivine:

$$a^{sp}_{MgAl_2O_4} = (X^{sp}_{Mg})(Y^{sp}_{Al})^2$$

where $(Y^{sp}_{Al}) = Al/Al + Cr + Fe^{3+}$

$$a^{ol}_{fo} = (X^{ol}_{Mg})^2$$

As plagioclase in these rocks is nearly pure anorthite, the activity coefficient can be set equal to unity; for plagioclase of more sodic compositions, the activity-composition data from Saxena (1973, Fig. 56) can be used. Activity of the pyroxene end members in the pyroxene solid-solution can be approximated on the basis of a two-site model as first advocated by Mueller (1961, 1962) and discussed in depth by Blander (1972) and Wood and Banno (1973), such that when enstatite is considered as being the molecule $Mg_2Si_2O_6$:

$$(a^{opx}_{en}) = (X^{opx}_{MgM1})\,(X^{opx}_{MgM2})$$

and for diopside:

$$(a^{cpx}_{di}) = (X^{cpx}_{CaM2})\,(X^{cpx}_{MgM1})$$

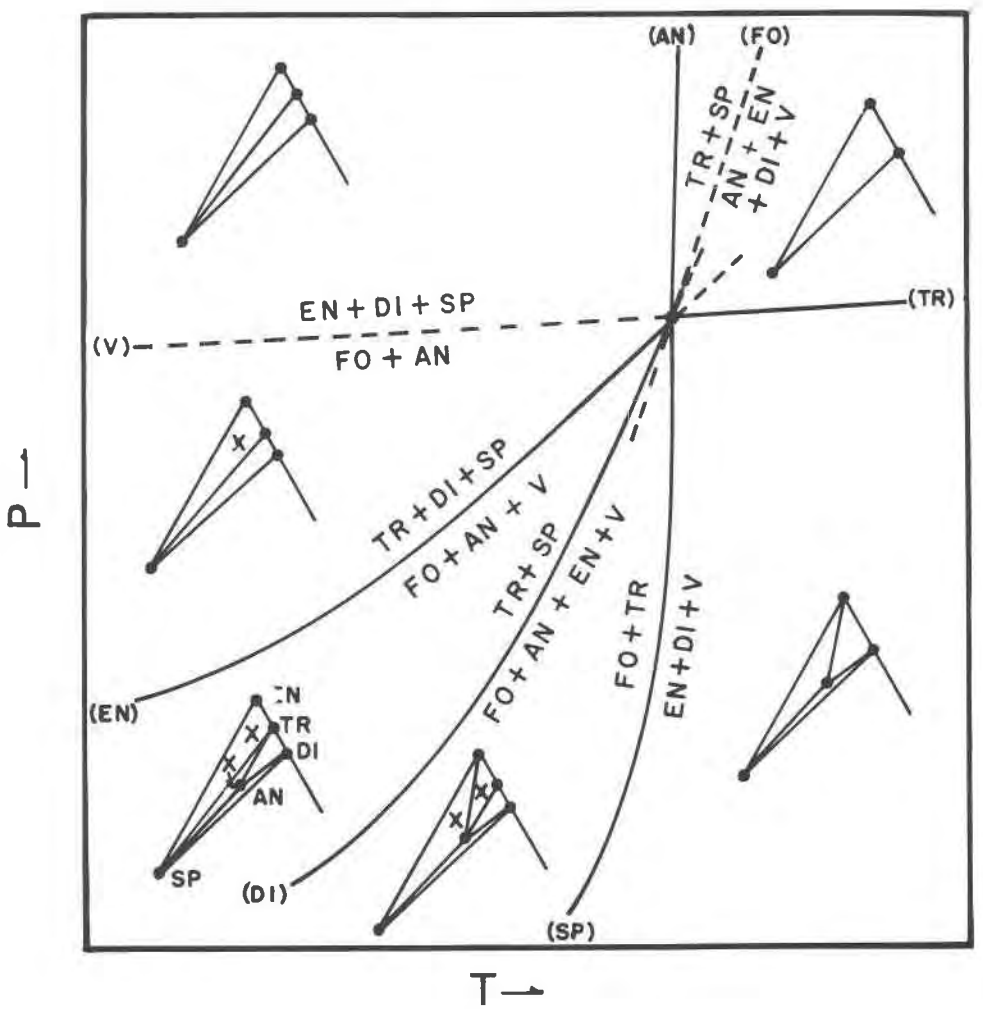

FIG. 8. *P-T* plot for the reactions governing the occurrence of plagioclase in the $CaO–MgO–Al_2O_3–SiO_2–H_2O$ system. An = anorthite, Di = diopside, En = enstatite, Fo = forsterite, Sp = spinel, Tr = tremolite, V = vapor, in this diagram H_2O. Chemographic diagrams show phase relations as projected from forsterite to the $CaO–Al_2O_3–SiO_2$ plane of the $CaO–MgO–Al_2O_3–SiO_2$ tetrahedron and are valid for olivine-bearing assemblages formed in an H_2O-saturated environment. *x* = assemblage found at Icicle Creek. *NOTE:* Reactions labeled (V) and (Fo) (dashed lines) are metastable in rocks of peridotitic composition in the presence of an H_2O-saturated vapor phase.

TABLE 7. Reactions governing the occurrence of anorthite in peridotite, Part I Amphibole considered as pure tremolite

Participating Phases

An = Anorthite, $CaAl_2Si_2O_8$
Di = Diopside, $CaMgSi_2O_6$
En = Enstatite, $MgSiO_3$
Fo = Forsterite, Mg_2SiO_4
Sp = Spinel $MgAl_2O_4$
Tr = Tremolite $Ca_2Mg_5(Si_8O_{22})(OH)_2$
V = Vapor, H_2O

Reactions

(V, Tr)	$2Fo + An = 2En + Di + Sp$
(Sp, An)	$Fo + Tr = 5En + 2Di + H_2O$
(Di)	$Tr + 2Sp = 2An + 3Fo + En + H_2O$
(Fo)	$2Tr + Sp = An + 8En + 3Di + 2V$
(En)	$2Tr + Di + 5Sp = 5An + 8Fo + 2V$

Thus the equilibrium constant becomes:

$$K = \frac{(X^{opx}_{MgM1})(X^{opx}_{MgM2})(X^{cpx}_{MgM1})(X^{cpx}_{CaM2})(X^{sp}_{Mg})(Y^{sp}_{Al})^2}{(X^{ol}_{Mg})^4(X^{plag}_{an})} \quad (2)$$

The next problem is in determining how to apply this value for the equilibrium constant to calculations pertaining to the pressure of equilibrium. The expression for log K as a function of P and T from Bacon and Carmichael (1973) yields unrealistically low pressures for the Icicle Creek rocks (*e.g.* − 3.9 kilobars for rock I-26). This error is probably due to the fact that, as vapor-free reactions such as this have small values of ΔS, they are sensitive to small errors in the thermochemical data. The error in determinations of entropy and enthalpy for the participating phases can be eliminated if the equilibrium pressure can be estimated at 715°C.

If the equilibrium pressure is known at a given temperature, the dependance of the equilibrium constant on pressure can be derived from the following relation:

$$d\ \ln K / dP = -\Delta V/RT$$

The resulting expression for the forsterite–anorthite reaction is:

$$-\log K = 0.1025\,(P_1 - P_2)/T \quad (3)$$

where $0.1025 = -\Delta V/2.303R$, P_1 = equilibrium pressure when $\log K = 0$, and P_2 = equilibrium pressure when $\log K \neq 0$.

Extrapolation of unpublished work of Windom (personal communication) shows that the reaction forsterite + anorthite = enstatite + diopside + spinel occurs at about 6.4 kilobars at 715°C, a value which is within 0.2 kilobars of that extrapolated from the work of Kushiro and Yoder (1966). This can be considered as P_2, with a hypothetical P_1 existing at a pressure where $K = 1.0$. In the pure system the only substitutions which can affect the equilibrium constant are those by which aluminum dissolves in the pyroxenes and enstatite dissolves in diopside. At these low temperatures the substitution of calcium in enstatite can be considered to be negligible. Assuming that the iron content of the pyroxene does not affect the aluminum content and that, as there is no jadeite component in the clinopyroxene, aluminum will dissolve equally into orthopyroxene and clinopyroxene, the aluminum content of the pyroxenes coexisting with olivine, spinel, and plagioclase can be estimated from analyses in Table 2. Orthopyroxenes from rocks containing green spinel have an $X^{opx}_{AlM1} = 0.06$ (*e.g.* # 3, Table 2). X^{cpx}_{CaM2} can be estimated from Figure 5 to be about 0.98 in the pure system at 715°C. By combining these values with equations (2) and (3) and solving for P_1 at a temperature of 715°C, we get $P = 6.8$ kilobars when $K = 1.0$.

Equation (2) indicates that the largest effect on the equilibrium pressure will be caused by the dilution of aluminum in spinel. Thus in a $P-Y^{sp}_{Al}$ diagram the pressure of equilibrium for the reaction forsterite + anorthite = enstatite + diopside + spinel will fall with decreasing aluminum in the spinel. This curve can be calculated with the information now available, assuming for this model that the ion substituting for aluminum in spinel is chromium, as chromium is far more abundant in spinel from high-grade ultramafics than ferric iron (Evans and Frost, 1975).

First the activity of anorthite in plagioclase can be assumed to be unity, as plagioclase from all olivine–plagioclase rocks is nearly pure anorthite. Second, by specifying the iron content of the olivine, the iron content of the other participating phases can be calculated from using the previously determined K_d values. For example: let $X^{ol}_{Mg} = 0.85$, about mid-way in the composition range of olivine from Icicle Creek. From K_d between olivine and enstatite, X^{opx}_{Mg} can be determined as 0.862. K_d between $M1$ and $M2$ sites in orthopyroxene can be calculated from the data of Saxena and Ghose (1971) to be 7.0 (Stroh, personal communication) at 715°C. From this, the site occu-

pancy can be calculated as: $X^{opx}_{MgM1} = 0.958$, $X^{opx}_{MgM2} = 0.765$. From Figure 4 it can be determined that at these temperatures, diopside coexisting with enstatite with an $X^{opx}_{Mg} = 0.862$ should have $X^{cpx}_{Mg} = 0.925$ and $X^{cpx}_{CAM2} = 0.94$. Assuming that that portion of the $M2$ site not occupied by calcium contains iron, then $X^{cpx}_{MgM1} = 0.98$. When one varies the aluminum content of spinel in this system, the Fe^{2+} content of it will also vary. Assuming that $Y^{sp}_{Fe^{2+}} = 0.05$, the expression for the dependence of K_d between olivine and spinel on Y^{sp}_{Al} can be expressed as $K_d^* = \exp(0.85 - 2.94\ Y^{sp}_{Cr})$ (Evans and Frost, 1975).

With these data, using equations (2) and (3) and $P_1 = 6.8$ kilobars and calculating P_2 for various values of Y^{sp}_{Al}, the solid line in Figure 9 can be generated.

As noted on Figure 6, spinels from the hornblende–plagioclase peridotite have Y^{sp}_{Al} of 0.58 or greater, whereas those in the tremolite–enstatite–diopside–spinel hornfelses have Y^{sp}_{Al} of 0.39 or less. The range of these values and the pressure bracket, 2–4 kilobars, are shown as the cross-hatched rectangle in Figure 9. This indicates the area in which the reaction should occur according to the field data. The large discrepancy, a minimum of 2 kilobars, between the observed relations and those predicted by thermodynamic calculations could be due to three causes, namely, error in the location of the reaction in the pure system, error in estimating the location of the box bracketing the pressure and spinel composition, and error in the model of thermodynamic activities.

It is conceivable that there is some error in the location of $P_{equilibrium}$ at $Y^{sp}_{Al} = 1.0$, but it probably is not much greater than ± 0.5 kilobar. Although there seems to be conflicting results in experimental determinations, they agree more than is generally recognized. Discounting those experiments which used natural olivine–plagioclase pairs, the only experimental work which does not agree with the results of Kushiro and Yoder (1966) and Windom (personal communication) is that of Herzberg (1972). However, data from that study are internally conflicting, and therefore the results are not reliable.

The bracketing spinel compositions on Figure 9 seem to be fairly well substantiated. They come from spinels which clearly occur in assemblages formed on either side of the reaction forsterite + anorthite = enstatite + diopside + spinel. Some question could be made about the presence of spinels of varying composition within individual samples of hornblende–plagioclase peridotite and whether they imply

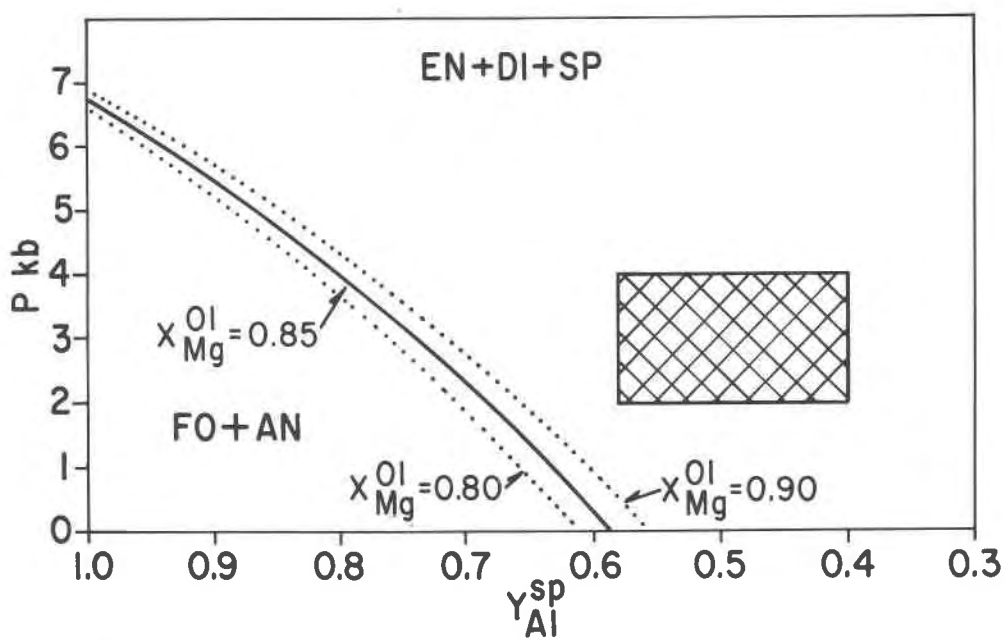

FIG. 9. The effect of spinel composition on the reaction forsterite + anorthite = enstatite + diopside + spinel in an iron-bearing system. An = anorthite, Di = diopside, En = enstatite, Fo = forsterite, Sp = spinel. Cross-hatched box indicates the range of spinel compositions and pressures at which the reaction seems to take place at Icicle Creek. $T = 715°C$.

TABLE 8. Reactions governing the occurrence of anorthite in peridotite, Part II Amphibole with variable composition

Participating Phases

An = Anorthite, $CaAl_2Si_2O_8$
Di = Diopside, $CaMgSi_2O_6$
En = Enstatite, $MgSiO_3$
Fo = Forsterite, Mg_2SiO_4
Hb = Hornblende, $Na_{.15x}\ Ca_2Mg_5 - {}_{.85x}(Si_8 - {}_xAl_xO_{22})(OH)_2$
Sp = Spinel, $MgAl_2O_4$
V = Vapor, $H_2O + (.075x)\ Na_2O$

Reactions, where x = the amount of Al^{IV} in Hb.

(V, Hb*) $2Fo + An = 2En + Di + Sp$

(An*) $Hb + (1 + .775x)\ Fo = (5 - .225x)\ En + 2Di + .925xSp + V$

(Sp*) $Hb + (1 - 1.075x)\ Fo = (5 - 2.075x)\ En + (2 - .925x)\ Di + .925x\ An + V$

(Di*) $Hb + (2 - .925x)\ Sp = (3 - .775x)\ Fo + (1 - .225x)\ En + 2An + V$

(Fo*) $2Hb + (1 - 1.075x)\ Sp = (8 - 2.00x)\ En + (3 - .775x)\ Di + (1 + .775x)\ An + 2V$

(En*) $2Hb + (1 - .225x)\ Di + (5 - 2.07x)\ Sp = (8 - 2.00x)\ Fo + (5 - .225x)\ An + 2V$

disequilibrium. Similar ranges in spinel composition from chlorite–forsterite–enstatite–spinel rocks were interpreted by Evans and Frost (1975) as being due to local equilibrium caused by limited mobility of Al_2O_3. The same explanation is valid for the rocks from Icicle Creek, but as the reaction responsible for this variation, tremolite + spinel = forsterite + anorthite +enstatite+H_2O, will proceed with a continual depletion of aluminum in the spinel, it is the more aluminous spinels which are out of equilibrium with the rock assemblage, not the more chromiferous ones.

The third source of error is in the assumptions used in the thermodynamic calculations. As the reaction has a very small dP/dT, even if the temperature value of 715°C was off by 20°, it would affect the results only by a factor of 2 percent. The assumption that $\Delta V_{298,1} = \Delta V_{988,P}$ also adds an error of about 2 percent. The other major error in the thermodynamics is involved in modeling the activity of various components in the participating phases, particularly the pyroxenes and spinel. The model used for the pyroxenes does not take into account the minor substitutions of Al, Cr, Fe^{3+}, or Na, but these would only tend to decrease the activity of the magnesium end members in the pyroxenes and hence increase the difference seen in Figure 9. As all the above errors are relatively small compared to the observed discrepancy, the expression for the activity of $MgAl_2O_4$ in spinel seems to be the major culprit.

There seems little doubt that the two-site model for the activity of various end members in the spinel solid-solution is valid. First described by Irvine (1965), it assumes that Fe^{2+}, Fe^{3+}, Mg, Al, and Cr each substitute independently in the spinel structure. In the more recent model of Gooley *et al.* (1974) it is assumed that $FeCr_2$ substitutes ideally for $MgAl_2$. As there is no charge constraint on the substitution pattern, this is an unreasonable assumption, and therefore the model of Irvine (1965) is preferred.

Stroh (personal communication) found that the two-site model works reasonably well in calculations on the reaction $MgAl_2Si_2O_6 + Mg_2SiO_4 = Mg_2Si_2O_6 + MgAl_2O_4$ for rocks which formed at high temperatures, but rather poorly for those from Paddy-Go-Easy Pass and Icicle Creek, which formed at rather low temperatures. As there is clearly immiscibility within the spinel tetrahedron at metamorphic temperatures (Turnock and Eugster, 1962), it would be reasonable to assume that, although the substitution of chromium for aluminum in the spinel structure may be nearly ideal at magmatic temperatures, there should be increasing deviation from ideality with decreasing temperature. It appears that it is this nonideality which is producing the discrepancy seen in Figure 9.

Effect of changes in hornblende composition on the topology of the plagioclase-forming reactions

A source of possible error inherent in interpreting Figure 8 is that changes in topology could be associated with the fact that the amphibole involved in the reactions is not tremolite. In order to estimate the effect of amphibole composition on the topology, a Schreinemakers' analysis was made on the invariant point in Figure 8 using a variable hornblende composition.

By coupling the reaction controlling the hornblende composition (reaction (1)) with reaction (Sp, An) in Table 7, and solving so that tremolite is eliminated, reaction (An*) (Table 8) is produced. Then by coupling reaction (An*) with (Hb, V*), the rest of the reactions on Table 8 can be generated. The addition of Na_2O to the system does not add another phase. Since the alkali is dissolved in hornblende on one side of the reaction and in the fluid phase on the other, the reactions on Table 8 are divariant. However, if Al^{IV} in hornblende is specified, the reactions become univariant and their intersection becomes invariant in a P-T plane.

If Al^{IV} in hornblende is allowed to vary from 0.0 to 2.4, with 2.4 being nearly the limit for natural horn-

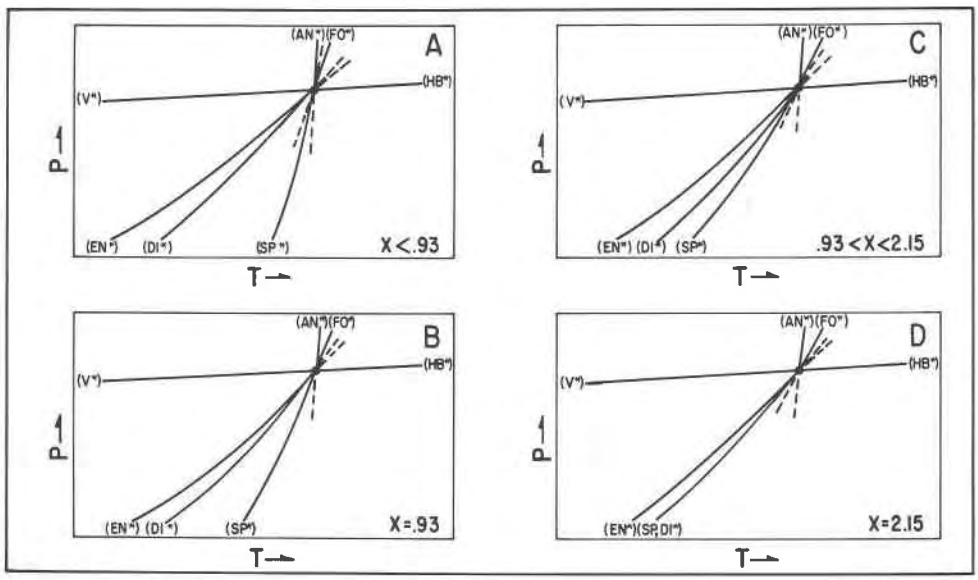

FIG. 10. A series of *P-T* sections through *P-T*-composition space. The compositional variable, x, is the value of Al^{IV} in the hornblende. The reactions shown are those listed in Table 8. The diagrams show the changes in topology associated with changes in hornblende composition assuming that the hornblende composition changes according to the solid line in Figure 7.

blendes, then some of the coefficients on Table 8 will change from a positive value through 0.0 to a negative value. In other words, the phase will become a product instead of a reactant. For example, in the reaction labeled (Fo*), the coefficients for spinel become 0 at $x = 0.93$. At that value the reaction would be labeled (Fo, Sp*). Clearly, at this same value of x, the coefficients for forsterite in reaction (Sp*) will also equal 0.0, and the stoichiometry for the two reactions will be the same. At values of x greater than 0.93, spinel will be on the opposite side of the reaction to which it is written on Table 8. Topologically, for values of Al^{IV} in hornblende of less than 0.93, stable (Fo*) is to the right of the metastable extention of (Sp*) (Fig. 10A). When $x = 0.93$, (Fo*) is colinear with (Sp*) (Fig. 10B), whereas for x greater than 0.93, (Fo*) is to the left of the metastable extention of (Sp*) (Fig. 10C). The point in Figure 10 where the sequence of *stable* reactions changes is that of diagram *D*, where the Al^{IV} content of hornblende is about 2.15. This value is well above that found in hornblende from Icicle Creek (Table 6), indicating that the topology for the naturally-occurring phases is essentially the same as that for the pure Na-free system (Fig. 8).

As the presence of sodium and aluminum in the amphibole would tend to stabilize it relative to other phases, it seems likely that the equilibrium temperature for the amphibole-breakdown reactions would increase with increasing Al^{IV} in the hornblende. In other words, the hornblende composition will become buffered by the system, and the hornblende will become progressively more aluminous as the reaction proceeds. The majority of the samples of hornblende–plagioclase peridotite from Icicle Creek seem to represent rocks which were buffered along the divariant reaction surface (Di*), as they contain the assemblage forsterite–hornblende–anorthite–enstatite–spinel, which would be divariant in the Na_2O–CaO–MgO–Al_2O_3–SiO_2–H_2O system. Similar buffering along (En*) was not observed as it would require a composition more calcic than that found in most metamorphosed blackwall rocks.

It should be noted, however, that the reactions on Table 8 and Figure 10 are not valid for all natural systems, as hornblende compositions could be buffered along different trends depending upon differences in coexisting phases or intensive variables. For example, hornblende buffered by reactions (Fo*) or (Sp*) might have entirely different compositions from those occurring along (En*) even if they formed at similar temperatures and pressures, as forsterite and spinel are essential for fixing a low activity of silica or a high activity of aluminum, respectively, in a coexisting hornblende. The reaction (Sp*) would be particularly complex, for with the constraint of spinel

saturation removed from the assemblage, albite might form in the plagioclase, adding an extra degree of freedom to the assemblage forsterite–enstatite–plagioclase–hornblende–diopside. However, these added complexities do not change the basic topology shown in Figure 8, which indicates that there is a divariant region in which olivine, anorthite, enstatite, and hornblende can coexist.

Conclusions

The major conclusion that can be drawn from this work is that the transition from the plagioclase–peridotite field to that of spinel–peridotite is strongly compositionally dependent. The transition, which is univariant in the $CaO–MgO–Al_2O_3–SiO_2$ system, becomes divariant or multivariant with the addition of other components, particularly NaO, Cr_2O_3, FeO, or Fe_2O_3. Some of the apparent discrepancies in experimental results can be accounted for on this basis. The experiments of Green and Hibberson (1970) and Emslie (1970) were done with other components present, particularly sodium, and the differences between their results and those of Kushiro and Yoder (1966) and Windom (personal communication) should not be surprising. Furthermore, as most natural peridotites are fairly poor in sodium and contain minor-to-significant amounts of chromium and iron (both of which are concentrated in spinel), the transition from plagioclase- to spinel–peridotite can take place in natural peridotites at pressures lower than those indicated experimentally. Thus, the occurrence of spinel, even one rich in aluminum, is not necessarily prima facie evidence for high-pressure, mantle origin for that rock.

Figure 11 gives a rough revision of O'Hara's (1967b) facies diagram for the $CaO–MgO–Al_2O_3–SiO_2–H_2O$ system at low pressures and high temperatures. Before discussing this figure it is best to stress again that the bulk rock composition will have a large effect, both on the relative location of the curves in the *P-T* plane, and on the variance of the transition boundaries, when applied to natural rocks. The low-temperature limit for the hornblende–spinel peridotite is shown here as being the reaction chlorite = forsterite + enstatite + spinel $+H_2O$. Below this reaction the rocks are referred to as metaperidotites, for if a rock has an equilibrium chlorite-bearing assemblage its origin as a result of crustal metamorphism is usually obvious. Whether the field of hornblende–spinel peridotite is truncated at high pressures by the crossing of the reactions chlorite = forsterite + enstatite + spinel + H_2O and forsterite + tremolite = enstatite + diopside + H_2O, as is suggested by forsterite–enstatite–diopside–chlorite rocks from the Alps (Evans and Trommsdorff, 1974) is not clear as yet. As noted above, the occurrence of a field of hornblende–plagioclase peridotite between those of hornblende–spinel peridotite and plagioclase lherzolite seems to be valid even in fairly aluminous systems.

Figure 11 can also be used to explain some coronas commonly found between olivine and plagioclase in gabbro and anorthosite. The sequences olivine–clinopyroxene–hornblende + spinel–plagioclase and olivine–orthopyroxene–hornblende + spinel–plagioclase have both been described in the literature (Shand, 1945; Murthy, 1958). Recently, similar coronas have been described from gabbroic rocks which have undergone no major metamorphism (Irvine, 1974; Nishimori, 1974). These coronas seem to represent reactions similar to (En*) and (Di*) in Table 8 and probably reflect local reequilibration of the assemblage forsterite + anorthite under retrograde, hydrous conditions.

Conclusions bearing on the validity of thermodynamic calculations involving spinel are also significant. It has been shown here that the use of the reaction forsterite + anorthite = enstatite + diopside + spinel as a geobarometer is fraught with difficulties, not the least of which is the problem of defining the activity of end members in the spinel solid-solution series. Expressions using thermochemical constants for the participating phases (*cf.* Bacon and

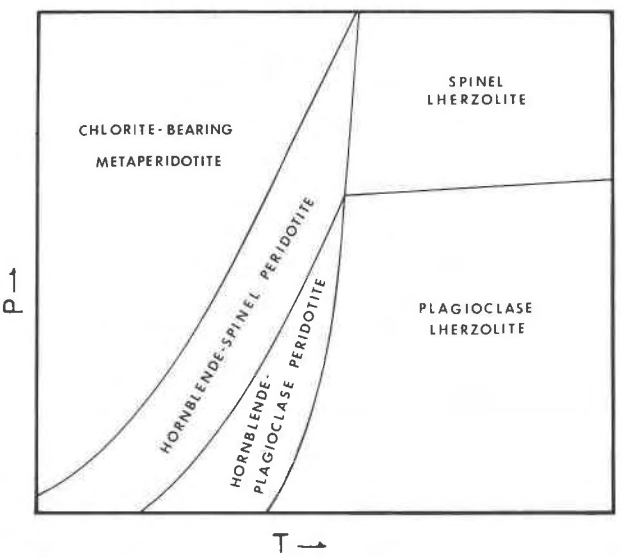

FIG. 11. Mineral facies in aluminous peridotite at pressures of less than about 10 kilobars and temperatures above 700°C.

Carmichael, 1973) contain far too much inherent error to make them applicable to geologic problems dealing with vapor-free reactions. Thus, even with adequate expressions for the activity of the components in the participating phases, the reaction can only be used as a geobarometer through careful applications of thermodynamics to an experimentally determined curve.

Acknowledgments

The author would like to thank the following individuals for their assistance in this project:

Wasant Pongsapich who first alerted me to the occurrence of high-grade ultramafic hornfelses in the Icicle Creek valley.

Robert Vocke and John Kramer who assisted in the field work and carried rocks.

Bernard W. Evans, I. S. McCallum, J. M. Rice, and B. W. D. Yardley whose criticisms markedly improved the quality of this manuscript.

I would also like to acknowledge N.S.F. grant # GA 29767 (Evans) for financial assistance during the course of this study.

References

ALMOND, D. C. (1964) Metamorphism of tertiary lavas in Strathaird, Skye. *Trans. R. Soc. Edinburgh,* **65,** 413–434.

BACON, C. R. AND I. S. E. CARMICHAEL (1973) Stages in the *P-T* path of ascending basalt magma: an example from San Quintin, Baja California. *Contrib. Mineral. Petrol.* **41,** 1–22.

BARKER, F. (1964) Sapphirine-bearing rock, Val Codera, Italy. *Am. Mineral.* **49,** 146–152.

BLANDER, M. (1972) Thermodynamic properties of orthopyroxene and clinopyroxene based on the ideal two-site model. *Geochim. Cosmochim. Acta,* **36,** 787–799.

BROWN, G. M. (1956) The layered ultramafic rocks of Rhum, Inner Hebrides. *Phil. Trans. R. Soc. London, Ser. B,* **240,** 1–53.

CHALLIS, G. A. (1965) The origin of New Zealand ultramafic intrusions. *J. Petrol.* **6,** 322–364.

CHINNER, G. A. AND T. R. SWEATMAN (1968) A former association of enstatite and kyanite. *Mineral. Mag.* **36,** 1052–1060.

EMSLIE, R. F. (1970) Liquidus relations and subsolidus reactions in some plagioclase-bearing systems. *Carnegie Inst. Wash. Year Book,* **69,** 148–155.

EVANS, B. W. AND B. R. FROST (1975) Chrome-spinel in progressive metamorphism—a preliminary analysis. *Geochim. Cosmochim. Acta,* **39,** 959–972.

——— AND V. TROMMSDORFF (1974) Stability of enstatite + talc and CO_2-metasomatism of metaperidotite, Val d'Efra, Lepontine Alps. *Am. J. Sci.* **274,** 274–296.

FAWCETT, J. J. AND H. S. YODER (1966) Phase relationships of chlorites in the system $MgO–Al_2O_3–SiO_2–H_2O$. *Am. Mineral.* **51,** 353–380.

FROST, B. R. (1973) *Contact Metamorphism of the Ingalls Ultramafic Complex at Paddy-Go-Easy Pass, Central Cascades, Washington.* Ph.D. Thesis, University of Washington, Seattle, Washington.

——— (1975) Contact metamorphism of serpentinite, chloritic blackwall, and rodingite at Paddy-Go-Easy Pass, Central Cascades, Washington. *J. Petrol.* **16,** 272–313.

GOOLEY, R., R. BRETT, J. WARNER AND J. R. SMYTH (1974) A lunar rock of deep crustal origin: sample 76535. *Geochim. Cosmochim. Acta,* **38,** 1329–1340.

GREEN, D. H. (1964) The petrogenesis of the high-temperature peridotite intrusion in the Lizard area, Cornwall. *J. Petrol.* **5,** 134–188.

——— AND W. HIBBERSON (1970) The instability of plagioclase in peridotite at high pressures. *Lithos,* **3,** 209–221.

HERZBERG, C. T. (1972) Stability fields of plagioclase- and spinel-lherzolite. *Prog. Experimental Petrol.* **2,** 145–148.

HESS, P. C. (1969) The metamorphic paragenesis of cordierite in pelitic rocks. *Contrib. Mineral. Petrol.* **24,** 191–207.

IRVINE, T. N. (1965) Chromian spinel as a petrogenetic indicator. Part 1—Theory. *Can. J. Earth Sci.* **2,** 648–674.

——— (1974) Petrology of the Duke Island Ultramafic Complex, Southeastern Alaska. *Geol. Soc. Am. Mem.* **138.**

——— AND G. H. SMITH (1967) The ultramafic rocks of the Muskox intrusion, Northwest Territories, Canada. In, P. J. Wyllie, Ed. *Ultramafic and Related Rocks.* John Wiley and Sons, New York. p. 38–49.

KNORRING, O. VON, T. G. SAHAMA AND M. LEHTINEN (1969) Kornerupine-bearing gneiss from Inanakafy near Betroka, Madagascar. *Bull. Geol. Soc. Finland* **41,** 79–84.

KRETZ, R (1961) Some applications of thermodynamics to coexisting minerals of variable composition. Example: orthopyroxene–clinopyroxene and orthopyroxene–garnet. *J. Geol.* **69,** 361–387.

KUSHIRO, I. AND H. S. YODER (1966) Anorthite–forsterite and anorthite–enstatite reactions and their bearing on the basalt–eclogite transformation. *J. Petrol.* **7,** 337–362.

LEAKE, B. E. (1960) Compilation of chemical analyses and physical properties of natural cordierite. *Am. Mineral.* **45,** 282–298.

——— (1964) New light on the Dawros Peridotite, Connemara, Ireland. *Geol. Mag.* **101,** 63–75.

——— (1971) On aluminous and edenitic hornblendes. *Mineral. Mag.* **38,** 389–407.

LINDSLEY, D. H., H. E. KING AND A. C. TURNOCK (1974) Composition of synthetic augite and hypersthene coexisting at 810°C: application to pyroxenes from lunar highlands rocks. *Geophys. Res. Lett.* **1,** 134–136.

LONEY, R. L., G. R. HIMMELBERG AND R. G. COLEMAN (1971) Structure and petrology of the alpine-type peridotite at Burro Mountain, California, U.S.A. *J. Petrol.* **12,** 245–309.

MACGREGOR, A. C. (1931) Scottish pyroxene–granulite hornfelses and the Odenwald beerbachites. *Geol. Mag.* **68,** 506–521.

MACGREGOR, I. D. (1974) The system $MgO–Al_2O_3–SiO_2$: Solubility of Al_2O_3 in enstatite for spinel and garnet peridotite compositions. *Am. Mineral.* **59,** 110–119.

MATTHES, S. (1971) Die ultramafischen Hornfelse, inbesondere ihre Phasenpetrologie. *Fortsch. Mineral.* **48,** 109–127.

MEDARIS, L. G. (1972) High-pressure peridotites in southwestern Oregon. *Geol. Soc. Am. Bull.* **83,** 41–57.

MISCH, P. (1966) Tectonic evolution of the northern Cascades of Washington State. In, H. C. Gunning, Ed. *Tectonic History and Mineral Deposits of the Western Cordillera. Can. Inst. Min. Metall. Spec. Pap.* **8,** 101–148.

MUELLER, R. F. (1961) Analysis of relations among Mg, Fe, and Mn in certain metamorphic minerals. *Geochim. Cosmochim. Acta,* **25,** 267–296.

——— (1962) Energetics of certain silicate solid solutions. *Geochim. Cosmochim. Acta,* **26,** 581–598.

MURTHY, M. V. N. (1958) Coronites from India and their bearing on the origin of coronas. *Geol. Soc. Am. Bull.* **69,** 23–38.

NISHIMORI, R. K. (1974) Cumulate anorthosite gabbros and peridotites and their relation to the origin of the calc-alkaline trend of the Peninsular Ranges Batholith (abstr.) *Geol. Soc. Am. Abstr. Progr.* **6,** 229.

O'HARA, M. J. (1967a) Mineral facies in ultrabasic rocks. In, P. J. Wyllie Ed. *Ultramafic and Related Rocks.* John Wiley and Sons, New York. p. 7–18.

——— (1967b) Mineral petrogenesis in ultrabasic rocks. In, P. J. Wyllie Ed., *Ultramafic and Related Rocks.* John Wiley and Sons, New York, p. 393–403.

ONUKI, H. (1965) Petrochemical research on the Horoman and Miyamori ultramafic intrusions, northern Japan. *Sci. Rep. Tohoku Univ. Ser. III,* **9,** 217–276.

ONYEAGOCHA, A. C. (1973) *Petrology and Mineralogy of the Twin Sisters dunite.* Ph.D. Thesis, University of Washington, Seattle, Washington.

PAPIKE, J. J., K. L. CAMERON AND K. BALDWIN (1974) Amphiboles and pyroxenes: characterization of *other* than quadrilateral components and estimates of ferric iron from microprobe data. *Geol. Soc. Am. Abstr. Progr.* **6,** 1053–1054.

PETERS, T. (1968) Distribution of Mg, Fe, Al, Ca, and Na in coexisting olivine, orthopyroxene, and clinopyroxene in the Totalp Serpentinite (Davos, Switzerland) and in Alpine metamorphosed Malenco Serpentinite (N. Italy). *Contrib. Mineral. Petrol.* **18, 65–75.**

PHILLIPS, E. R. (1959) An olivine-bearing hornfels from southeastern Queensland. *Geol. Mag.* **196,** 377–384.

——— (1961) An olivine-bearing hornfels from southeastern Queensland—a correction. *Geol. Mag.* **98,** 431–433.

PLUMMER, C. (1969) *Geology of the Crystalline Rocks, Chiwaukum Mountains and Vicinity, Washington Cascades.* Ph.D. Thesis, University of Washington, Seattle, Washington.

PONGSAPICH, W. (1974) *The Geology of the Eastern Part of the Mount Stuart Batholith, Central Cascades, Washington.* Ph.D. Thesis, University of Washington, Seattle, Washington.

REINHARDT, E. W. (1968) Phase relations in cordierite-bearing gneisses from the Gananoque area, Ontario. *Can. J. Earth Sci.* **5,** 455–482.

RICHARDSON, S. W. (1968) Staurolite stability in a part of the system Fe–Al–Si–O–H. *J. Petrol.* **9,** 467–488.

RICHEY, J. E. AND H. H. THOMAS (1930) The geology of Ardnamurchan, northwest Mull and Coll. *Geol. Surv. U.K. Mem.,* 393 p.

ROSS, C. S., D. M. FOSTER AND A. T. MYERS (1954) Origin of dunites and of olivine-rich inclusions in basaltic rocks. *Am. Mineral.* **39,** 693–737.

SAXENA, S. K. (1973) *Thermodynamics of Rock-Forming Crystalline Solutions.* Springer Verlag, New York.

——— AND S. GHOSE (1971) Mg^{+2}–Fe^{+2} order-disorder and the thermodynamics of the orthopyroxene solid crystalline solution. *Am. Mineral.* **56,** 532–559.

——— AND C. E. NEHRU (1975) Enstatite–diopside solvus and geothermometry. *Contrib. Mineral. Petrol.* **49,** 259–267.

SHAND, S. S. (1945) Coronas and coronites. *Geol. Soc. Am. Bull.* **56,** 247–266.

TROMMSDORFF, V. AND B. W. EVANS (1974) Alpine metamorphism of peridotitic rocks. *Schweizer. Mineral. Petrogr. Mitt.* **54,** 333–353.

TURNOCK, A. C. AND H. EUGSTER (1962) Fe–Al oxides: phase relations below 1,000°C. *J. Petrol.* **3,** 533–565.

WHITE, R. W. (1966) Ultramafic inclusions in basaltic rocks from Hawaii. *Contrib. Mineral. Petrol.* **12,** 245–314.

WOOD, B. J. (1973) Fe^{+2}–Mg^{+2} partition between coexisting cordierite and garnet—a discussion of the experimental data. *Contrib. Mineral. Petrol.* **40,** 253–258.

——— AND S. BANNO (1973) Garnet–orthopyroxene and orthopyroxene–clinopyroxene relationships in simple and complex systems. *Contrib. Mineral. Petrol.* **42,** 109–124.

ZEN, E-AN (1966) Construction of pressure-temperature diagrams for multicomponent systems after the method of Schreinemakers—a geometric approach. *U. S. Geol. Surv. Bull.* **1225.**